metals

MDPI

Article

Effects of X-rays Radiation on AISI 304 Stainless Steel Weldings with AISI 316L Filler Material: A Study of Resistance and Pitting Corrosion Behavior

Francisco Javier Cárcel-Carrasco *, Manuel Pascual-Guillamón and Miguel Angel Pérez-Puig

ITM, Universitat Politècnica de València, 46022 Valencia, Spain; mpascual@mcm.upv.es (M.P.-G.); mipepui@mcm.upv.es (M.A.P.-P.)

* Correspondence: fracarc1@csa.upv.es; Tel.: +34-963-87-7000; Fax: +34-963-87-9459

Academic Editor: Dhriti Bhattacharyya

Received: 17 February 2016; Accepted: 26 April 2016; Published: 29 April 2016

Abstract: This article investigates the effect of low-level ionizing radiation, namely X-rays, on the micro structural characteristics, resistance, and corrosion resistance of TIG-welded joints of AISI 304 austenitic stainless steel made using AISI 316L filler rods. The welds were made in two different environments: natural atmospheric conditions and a closed chamber filled with inert argon gas. The influence of different doses of radiation on the resistance and corrosion characteristics of the welds is analyzed. Welded material from inert Ar gas chamber TIG showed better characteristics and lesser irradiation damage effects.

Keywords: welding; radiation; dose; X-rays; pitting; corrosion; AISI 304; AISI 316L

1. Introduction

The objective of this study is to determine the effect of low intensity X-rays ionizing radiation on TIG-welds of AISI 304 stainless steel using AISI 316L as filler rods when a welding procedure modification is involved: TIG-conventional atmosphere and TIG in fully-chamber inert gas atmosphere. An analysis is made of the mechanical and microstructure properties and the effects produced by corrosion according to the radiation dose. Changes in the microstructure of a weld can change its behavior [1–3]. This article evaluates the weldability and micro-structural effects of ionizing radiation on AISI 304 stainless steel welded with a tungsten electrode and AISI 316L stainless steel filler material. The mechanical properties in response to corrosion are also examined.

This research analyses the effects of radiation on stainless steel components used in various applications, such as machines that produce radiation, elements subjected to radiation outside the atmosphere such as satellites and rockets, and nuclear waste containers. Microstructural changes can be produced in austenitic steels depending on the material and test conditions [4,5]. In verified studies, several methods have produced significant results in TEM microstructural analysis [4,6]. Test temperature, strains range, and the radiation dose are parameters that affect ductility in austenitic steels [7,8]. Various studies have also determined changes in the mechanical properties of materials in highly radioactive environments [9,10]. High intensity irradiation causes the hardening of metals, and causes small defects and dislocations in the structure during plastic deformation [11–15]. It has been shown that increased radiation is often accompanied by changes in the stress-strain curve with a variation of elasticity and reductions in strain hardening capacity [10]. However, these results are mostly seen for neutron irradiation and as the effects of X-ray irradiation have not yet been determined they are the subject of this study.

2. Materials Used and Experimental Procedures

2.1. Materials Used

AISI 304 stainless steel is widely used in the chemical, organic liquids, aeronautical, naval, power generation, nuclear industries, as well as in construction, pharmaceutical and food handling, and transport. It is also used in cutlery, sinks, pipe-lines, vessels, tanks, elevator rendering and many other applications. AISI 316L stainless steel is widely used in the chemical and petrochemical industry. It is used as a filler material in welding and due to its low carbon content prevents the formation of chromium carbide at the grain boundaries. Both chemical compositions are shown in Table 1. The test specimens were prepared from plates of AISI 304 stainless steel measuring 180 mm in length, 75 mm in width, and 1.5 mm thick; and with dimensions once welded of 180 mm in length, 150 mm in width, and 1.5 mm thick.

Table 1. Composition of stainless steel (SS) and welding filler (WF).

ASTM	EN10088-2	%C	%Cr	%Ni	%Mn	%Si	%Mo
304 (SS)	X5CrNi18-10	0.07	18	9.5	1.90	1.00	-
316L (WF)	X2CrNiMo17-12-2	0.04	17–20	11–14	2.50	0.90	2.0–2.5

The joints were welded in two distinct approaches. The first was a conventional TIG-weld followed by air cooling in a conventional atmosphere. The second approach was a TIG-weld in an inert argon gas chamber made especially for this type of welding, shielded from that Ar atmosphere and weld cooling taking place into the chamber. Welding in the closed chamber filled with inert argon gas is presented in Figure 1. The welding parameters were: current 60 to 80 A, applied bias 21 V, argon flow rate 10 to 12 L/min; and a travel rate of 4 mm/s. To facilitate the process, the specimens were welded with a single bead. After sanding the bead, the specimens were mechanically cold cut to avoid any heat effect on the welds.

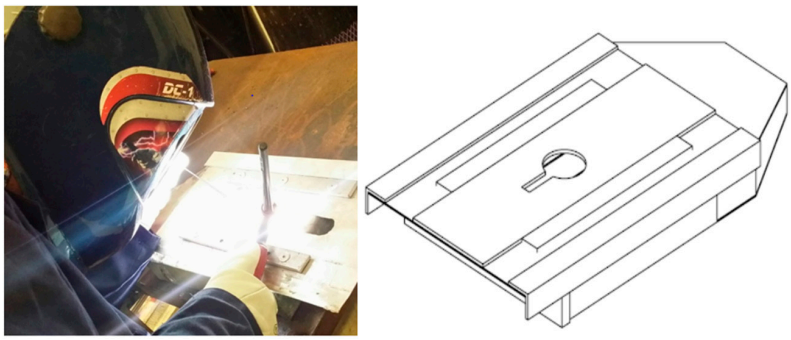

Figure 1. Inert gas chamber design (**right**) and welding process (**left**).

Three batches of welded specimens were irradiated with X-rays ionizing radiation doses of 200, 700, and 1000 Gy respectively. The fourth batch remained unirradiated (0 Gy). The radiation doses in all cases was measured in J/kg. In the international system the unity Sievert (Sv) is used for doses absorbed by living matter, and Gray (Gy) for any other type of material. The welded plates were irradiated inside the bunker which was specifically authorized and supervised by the Spanish Nuclear Safety Council (CSN, Madrid, Spain).

The specimens were TIG-welded in a conventional atmosphere or in an argon chamber. Twenty-four specimens were produced in total for each of the tests and the specimens measured 150 mm in length, 20 mm in width, and were 1.5 mm thick. The size of the specimens met the requirements described in UNE-EN 10002-1 corresponding to: Metallic materials. Tensile test, Part 1: Test methods at room temperature.

The researched welds were irradiated with different doses to study the evolution and behavior of materials under irradiation. The X-ray equipment operates at 200 KV maximum and 4.5 mA, and emits radiation at an angle of 40, although the welded plates were irradiated with 160 KV voltage and 3.5 mA at doses of 15 uninterrupted minutes to avoid overheating the unit.

The exposure time of the specimens after which we searched for the required radiation dose was as follows: 200 Gy-exposure time 35 h; dose of 700 Gy-exposure time 125 h; dose of 1000 Gy-exposure time 178 h. The device has been manually connected 428 times, 15 min each, for a total of 178 h of irradiation. Every week, it was radiated around 25 h. Welding was carried out in an inert and environmental atmosphere in order to be subsequently radiated and see the effects caused in both cases.

The welding parameters were 70 A, 20 V and 10 L/min of argon output nozzle. Approximately 200 mm/min was the welding speed.

2.2. Experimental Processes

Comparisons are made in terms of a microstructure, resistance, and corrosion for the AISI 304 steel welds made in different atmospheres with tungsten electrodes and AISI 316L filler. Tensile test: This test was carried out in concordance to UNE-EN 10002-1 standard tests. Mechanical properties: Tensile strength, yield strength, break strain and break energy were determined as indicative parameters of structural changes.

Microhardness test: To describe the influence of the different crystal structures we used a microhardness test according to UNE-EN 1043-2 standard. Microhardness was assessed in three different zones: the base material (BM) in the thermally affected zone (TAZ); the interface between TAZ and the zone with weld filler material (WZ), and the weld filler material zone (WZ).

The device used for microhardness testing is a vickers type, namely, a diamond pyramid type that in our case causes a small footprint when the order of 300 g loads is applied.

Pitting corrosion test: the welds were prepared by cutting and machining the specimens. One group of specimens was selected to determine the mechanical characteristics according to UNE-EN ISO 7348:2006 and UNE 112-029. Micrographs were obtained from a second group of specimens. A third group of specimens was put in a 10% ferric chloride solution for 72 h to observe the degree of corrosion suffered by the welds.

The speed at which the tensile test was done was 300 N/s. The samples were flat. The test specimens were prepared from plates of AISI 304 stainless steel measuring 180 mm in length, 75 mm in width, and 1.5 mm thick; and with dimensions once welded- 180 mm in length, 150 mm in width, and 1.5 mm thick.

3. Results and Discussion

The results presented in this work try to verify the influence of welding process on the behavior of the AISI 304 stainless steel TIG-welds made with ER AISI 316 L rods in conventional atmosphere and argon chamber; and subsequently subjected to ionizing radiation and evaluate the response to corrosion to learn how to prevent deterioration in aggressive environments.

3.1. Strength Properties

Data from tensile tests results are presented in Table 2. Materials welded in the Ar chamber attain better behavior because of its more favorables properties. That is because the Ar atmosphere is continuous in the chamber, it is filled up and its gas losses are supplied. The argon is too cold when it enters the chamber and has a great capacity to maintain and extract the welding heat. The Ar gas in the conventional procedure TIG is exposed to the environmental conditions, it could have stability protector steam and its cooling capacity is more restrictive. Yield and tensile strength of the irradiated welds tend to decrease until reaching a minimum when irradiation reaches 700 Gy and both strengths rise. The recovery part takes place for irradiation values of 1000 Gy. This has been generally verified in

all the test specimens. The break strain (ductility) and break energy (toughness) reduce continuously leading to embrittlement of irradiated weld samples, Table 2.

Table 2. Tensile Properties for radiation doses and types of welds.

Irradiated Doses	Conventional Atmosphere	Argon Chamber	Conventional Atmosphere	Argon Chamber
Dose (Gy)	Yield Strength (MPa)		Tensile Strength (MPa)	
0	378 ± 20	415 ± 14	569 ± 28	623 ± 21
200	376 ± 13	392 ± 19	551 ± 22	587 ± 29
700	372 ± 8	389 ± 9	544 ± 31	583 ± 14
1000	407 ± 10	411 ± 17	620 ± 30	616 ± 26
Dose (Gy)	Break Strain (%)		Break Energy (J)	
0	33 ± 7	51 ± 11	367 ± 23	673 ± 170
200	29 ± 6	38 ± 5	350 ± 53	475 ± 59
700	24 ± 10	32 ± 3	360 ± 90	388 ± 45
1000	30 ± 5	33 ± 5	401 ± 95	398 ± 60

At low radiation levels, the absorbed energy produces interatomic vibrations that increase defect formation in the network, mainly leading to vacancies. That causes reduction in the mechanical characteristics. Atomic motion grows with high doses of radiation and dislocations, and massive pinning is involved in the structure. The result was an increase in the strength characteristics and embrittlement when subjected to plastic deformation. The fractures were mostly ductile and generally occurred in the thermally affected zone (TAZ) at the interface between the AISI 304 steel plate and the AISI 316L filler material. The fractures occurred in this area because there are changes in the grain structure: recovery grain, diffusion of Mo, Ni and C, and probably some Mo-carbides precipitation to prevent the massively harmful precipitation of Cr-carbides [16–18].

3.2. Microhardness Test Results

Microhardness results are shown in Table 3. The maximum hardness is produced at the weld interface with an absorbed dose of 1000 Gy. There is little variation in hardness for the three radiation levels. It is evident that the area of the AISI 304 base metal is harder than the AISI 316L filler metal in the weld, as a result of a process similar to casting solidification. There is little variation between the hardness values produced by the two welding environments (conventional atmosphere and an argon chamber) as stainless steel generally hardens with deformation. However, very small differences in hardness were produced by variations in radiation dose.

Table 3. Hardness test results for different radiation doses and types of welding.

Dose (Gy)	Conventional Atmosphere	Argon Chamber	Conventional Atmosphere	Argon Chamber	Conventional Atmosphere	Argon Chamber
	TAZ Metal Base Zone		TAZ Interfac with Weld Zone		Weld Zone	
0	220 ± 5	220 ± 6	195 ± 9	202 ± 8	200 ± 9	203 ± 8
200	215 ± 8	218 ± 9	221 ± 9	190 ± 7	204 ± 9	202 ± 7
700	210 ± 10	214 ± 9	213 ± 8	189 ± 9	194 ± 8	200 ± 9
1000	230 ±9	223 ± 10	225 ± 10	215 ± 9	202 ± 10	230 ± 9

The results show that the increase in mechanical and resistant characteristics following irradiation at 1000 Gy produced a progressive embrittlement. The structure of the specimens after welding in two distinct environments and irradiation at the three distinct levels did not vary; and so the progressive embrittlement was the consequence of absorbed energy producing a change in the equilibrium positions of the atoms which, in turn, pinned dislocations. This increase in embrittlement may also be the consequence of increased corrosion as can be observed in the micrographs, Figures 2 and 3 and is especially noticeable in the specimens welded in a conventional atmosphere.

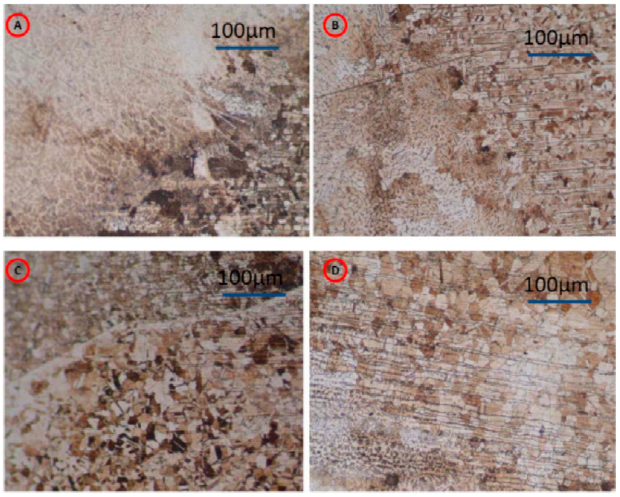

Figure 2. Microstructure of the weld made in conventional atmosphere, ×100. Interface weld zone—thermally affected zone (WZ-TAZ): (**A**) not irradiated; (**B**) at 200 Gy; (**C**) at 700 Gy; (**D**) at 1000 Gy.

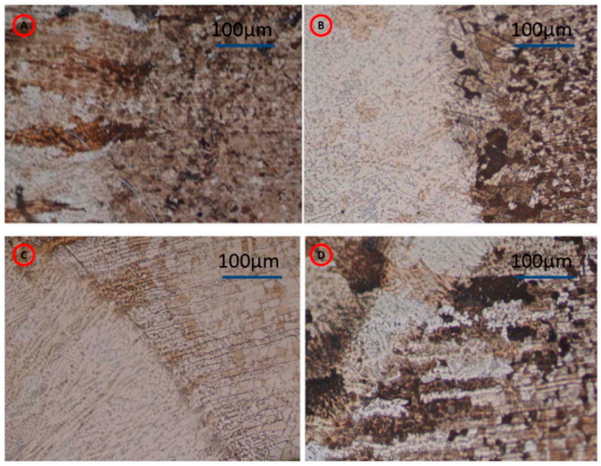

Figure 3. Microstructure of the weld made in an Ar chamber, ×100. Interface WZ-TAZ: (**A**) not irradiated; (**B**) at 200 Gy; (**C**) at 700 Gy; (**D**) at 1000 Gy.

Figure 2 shows weldings with the filler AISI 316L, the structure material is dentritic grain, which is characteristic for austenitic grain when we approach the thermally affected area. As you can see in the interface there are combinations between dentritic and austenitic grains and small formations of chromium carbide, which are fully austenitic in the thermally affected area but larger than the material base, where one can see a major presence of carbides of chrome compared to the interface, since this small appearance of carbides is a consequence of not being a total solubilization process. In Figure 3 there are structural variations and although the filler material and the area affected thermally are very similar to Figure 2, the grain size is smaller, as is the formation of carbides, in consequence of the total isolation from the atmospheric and environmental influence, which benefits the action of the influence of ionizing radiation improving both the corrosion and embrittlement, as the irradiated dose increases.

3.3. Characteristics of the Corrosion Pitting

The results regarding resistance to pitting corrosion are presented in Figure 4 for the specimens that were welded in a conventional atmosphere, and Figure 5 for the specimens welded in an argon atmosphere chamber. The corrosion aspects are related to the level of radiation. Specimens welded in the argon chamber were less corroded at 200 and 700 Gy irradiations. However, defects that occurred in the specimens exposed at 1000 Gy affected the grain microstructure due to embrittlement from

displacement caused by atomic vibration and pinned dislocations from the X-ray energy received. Little corrosion occurred at low irradiance levels, but corrosion increased markedly at higher levels. To quantify the results, the specimens were weighed before and after being subjected to 72 h of corrosion. The results showed that a pitting corrosion rate of 3.1×10^{-3} g/h occurred in the specimens welded by conventional TIG irradiated with 1000 Gy. A better result was reached with coupons welded in the chamber: 2.8×10^{-3} g/h.

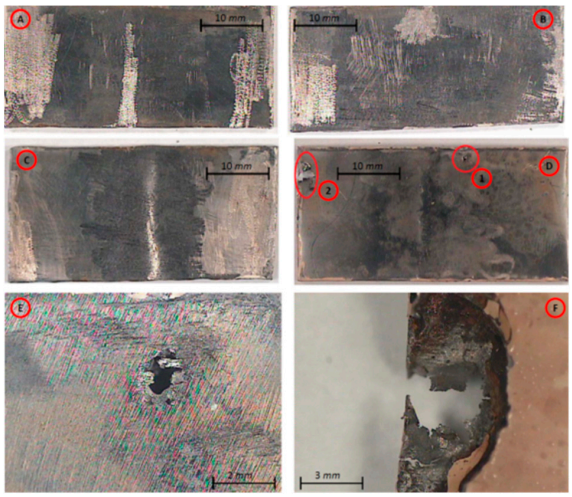

Figure 4. Pitting corrosion test of 304 stainless steel with 316L filler specimens welded in conventional atmosphere: (**A**) not-irradiated condition; (**B**) exposed to 200 Gy; (**C**) to 700 Gy; (**D**) to 1000 Gy; (E) defect 1 amplification from (**D**); (F) defect 2 amplification from (**D**).

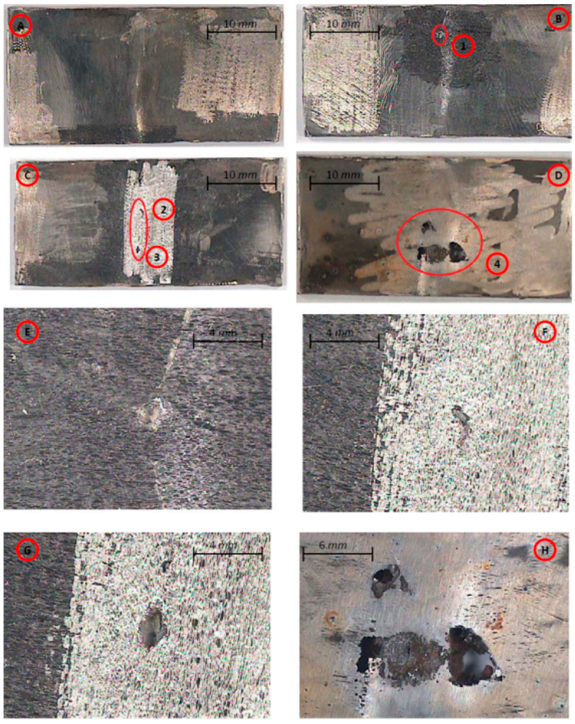

Figure 5. Pitting corrosion test of 304 stainless steel with 316L filler specimens welded in conventional atmosphere: (**A**) not-irradiated condition; (**B**) exposed to 200 Gy; (**C**) to 700 Gy; (**D**) to 1000 Gy; (**E**) defect 1 amplification from (**B**); (**F**) defect 2 amplification from (**C**); (**G**) defect 3 amplification from (**C**); (**H**) defect 4 amplification from (**D**).

For the specimens welded in a conventional atmosphere it was also found that the corrosion was less in the specimens irradiated at 200 and 700 Gy than at 1000 Gy. However, corrosion was lesser for specimens welded in the argon chamber and this was possibly because of a more uniform cooling in the argon chamber that produced more stable microstructure with smaller grains, less movement from atomic vibration and lesser dislocation density. Thus, it can be seen that corrosion increases with irradiation. At 200 and 700 Gy the corrosion is greater in specimens welded in a conventional atmosphere than in the argon chamber. However, corrosion also increased considerably for the argon chamber welded specimens when radiation levels reached 1000 Gy.

3.4. Analysis of Welded Microstructures

All micrographs from Figures 2 and 3 show three different areas: in the thermally affected zone (TAZ) the material area has a type of austenitic grain characteristic of stainless steel; in the interface area the austenitic grain combines with dendrite grains. The austenitic grain is larger here than in the base material area; and the weld zone (WZ) where the grain has solidified with a dendrite form is defined by a shape similar to the casting alloy. The solidification in the interface zone reveals a combination of equiaxed and dendritic grains with some chromium carbide precipitates at the grain boundary due to the AISI 316 L steel filler. In the TAZ near the weld, dendritic grains are larger than those in the base material due to the increased temperature in the welding process.

In the micrographs of the specimens with increased irradiation levels it is not possible to detect an embrittlement in the grain structure because of the radiation, and this effect is revealed in the variation in the resistance characteristics. In the welding of AISI 304 steel with 316L filler in the argon chamber it was possible to observe that the absorbed radiation affected both the mechanical and corrosion characteristics.

In the welding of AISI 304 steel + 316L with 200 Gy the minimal embrittlement of the material is revealed in the minimum yield and tensile strength, as well as the minimum hardness obtained in the Vickers microhardness test. In contrast, maximum intergranular and surface corrosion follows the absorption of 1000 Gy and this is probably due to variations in the embrittlement at the grain boundary limits. This confirms that radiation changes the material properties and that, as more radiation is absorbed, more embrittlement and corrosion occurs in the base material and weld.

Figures 6 and 7 indicate that the structural constituents are practically the same before and after irradiation. However, there is a variation in corrosion for irradiations at 200 Gy and 1000 Gy with a change in the atomic structure of the network generating defects at an interatomic level that change the mechanical and corrosive properties. Changes in spectrum signal of Ni, Mo and C appreciate, and so Mo carbide precipites while Cr remains in solid solution.

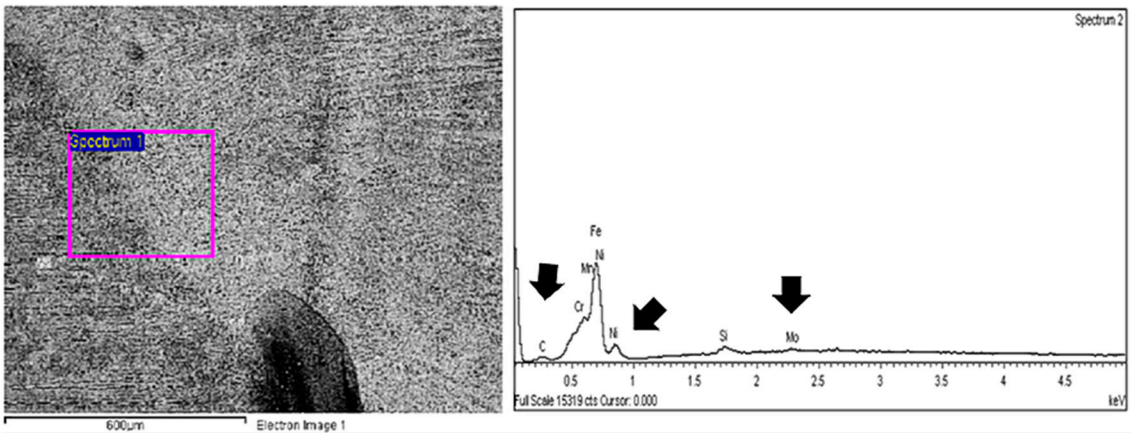

Figure 6. SEM spectrum and micrograph of the AISI 304 steel weld with AISI 316L filler welded in a conventional atmosphere and irradiated at 200 Gy.

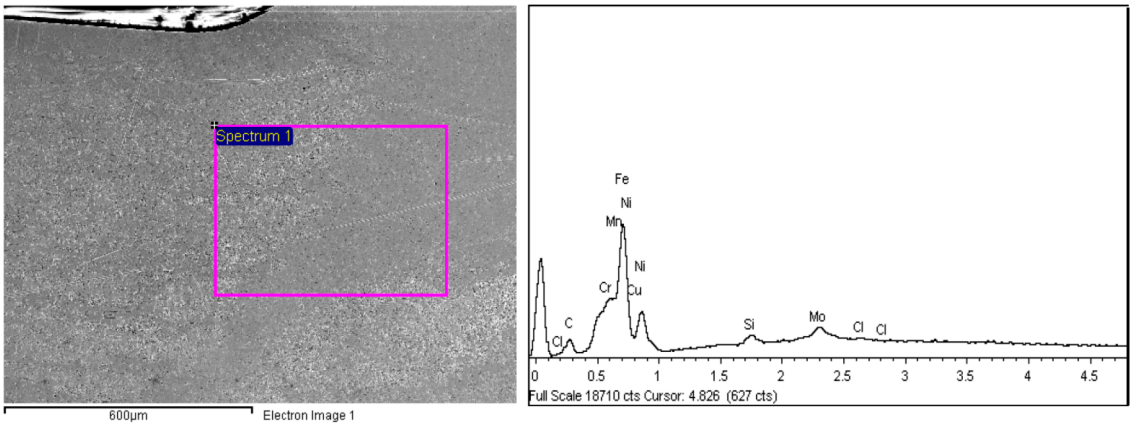

Figure 7. SEM spectrum and micrograph of the AISI 304 steel weld with AISI 316L filler welded in a conventional atmosphere and irradiated at 1000 Gy.

4. Conclusions

This study has shown that ionizing radiation varies the mechanical and structural properties of welds made in AISI 304 steel with 316L filler when welded in either a conventional atmosphere or an argon chamber.

A significant embrittlement of the material occurs following a dosage of 1000 Gy and this may be due to the absence of a constant cooling rate that would enable the grain structure to become more stable. One solution would be to weld in an inert argon chamber to protect the weld from sudden temperature changes. Given that the argon chamber maintains a constant cooling rate, welds made in the chamber revealed fewer differences in values for corrosion and resistance. A constant cooling rate may affect the grain structure so that it is more uniform and stable after irradiation due to less grain boundary embrittlement. Such material stability is essential for welding methods [19,20].

In general, welds subjected to doses of ionizing radiation have a reduced capacity to resist corrosion, and this is especially true for welds made in a conventional atmosphere. The microstrength tests showed that corrosion increased as irradiation increased, a tendency that was clearly seen when the dose was 1000 Gy or Sv.

Welds of AISI 304 steel made with 316L filler in a conventional atmosphere suffered the most corrosion. Given the convergence at high levels of irradiation it will be interesting in future studies to raise the irradiation levels.

Regarding the mechanical characteristics of the joints, the higher values of yield and tensile strength, strain and toughness are associated with the use of an argon chamber due to the protective effect of this atmosphere. Hardness shows a different behavior, with more similar values for both the samples welded at conventional atmosphere and at the argon chamber, and no clear conclusion can be extracted from the measurements, perhaps due to the statistical dispersion associated with those measures.

As shown in Table 2, the effect of an increment in the radiation dose received by the samples has a detrimental effect on the mechanical properties of the joint if the dose is less or equal to 700 Gy, but when the dose reaches 1000 Gy, this behavior changes and a notable recovery in all the mechanical properties is detected, with values that sometimes surpasses those of the samples not irradiated. The evolution of hardness shows the same tendency as the mechanical properties, with a loss of hardness until a dose of 700 Gy is reached and a recovery for doses of 1000 Gy. This result will trigger future research into high doses of radiation, relative to atomic vibrations and locks dislocations that may occur.

This behavior: a loss of properties until a certain dose of radiation is achieved. This is supposedly caused by an initial increase in vacancies population and a further embrittlement and increased hardness caused by dislocation pinnig. This effect is more significant in specimens welded in a conventional atmosphere than in an argon chamber.

Acknowledgments: We would like to give thanks to Language Translators Service of the Languishes Department of Universitat Politècnica de València, Spain.

Author Contributions: In this investigation, F.J.C.-C. and M.P.-G. conceived and designed the experiments; F.J.C.-C. and M.A.P.-P. performed the experiments; F.J.C.-C. and M.P.-G. analyzed the data; M.A.P.-P. contributed materials/analysis tools; F.J.C.-C. and M.P.-G. wrote the paper.

Conflicts of Interest: The authors declare no conflict of interest.

References

1. Lee, D.J.; Byun, J.C.; Sung, J.H.; Lee, H.W. The dependence of crack properties on the Cr/Ni equivalent ratio in AISI 304L austenitic stainless steel weld metals. *Mater. Sci. Eng. A.* **2009**, *513*, 154–159. [CrossRef]
2. Lee, D.J.; Jung, K.H.; Sung, J.H.; Kim, Y.H.; Lee, K.H.; Park, J.U.; Lee, H.W. Pitting corrosion behavior on crack property in AISI 304L weld metals with varying Cr/Ni equivalent ratio. *Mater. Des.* **2009**, *30*, 3269–3273. [CrossRef]
3. Gill, T.P.S.; Shankar, V.; Pujar, M.G.; Rodriguez, P. Effect of composition on the transformation of δ-ferrite TO σ in type 316 stainless steel weld metals. *Scr. Metall. Mater.* **1995**, *32*, 1595–1600. [CrossRef]
4. Lee, E.H.; Byun, T.S.; Hunn, J.D.; Yoo, M.H.; Farrell, K.; Mansur, L.K. On the origin of deformation microstructures in austenitic stainless steel: Part I—Microstructures. *Acta Mater.* **2001**, *49*, 3269–3276. [CrossRef]
5. Lee, E.H.; Byun, T.S.; Hunn, J.D.; Farrell, K.; Mansur, L.K. On the origin of deformation microstructures in austenitic stainless steel: Part II—Mechanisms. *Acta Mater.* **2001**, *49*, 3277–3287. [CrossRef]
6. Lee, E.H.; Byun, T.S.; Hunn, J.D.; Farrell, K.; Mansur, L.K. Origin of hardening and deformation mechanisms in irradiated 316 LN austenitic stainless steel. *J. Nucl. Mater.* **2001**, *296*, 183–191. [CrossRef]
7. Hertzberg, R.W. *Deformation and Fracture Mechanics of Engineering Materials*, 2nd ed.; John Wiley & Sons: Hoboken, NJ, USA, 1983.
8. Copley, S.M.; Kear, B.H. The dependence of the width of a dissociated dislocation on dislocation velocity. *Acta Metall.* **1968**, *16*, 227–231. [CrossRef]
9. Dai, Y; Egeland, G.W.; Long, B. Tensile properties of ferritic/martensitic steels irradiated in STIP-I. *J. Nucl. Mater.* **2008**, *377*, 115–221. [CrossRef]
10. Farrell, K.; Byun, T.S.; Hashimoto, N. Deformation mode maps for tensile deformation of neutron-irradiated structural alloys. *J. Nucl. Mater.* **2004**, *335*, 471–486. [CrossRef]
11. Wechsler, M.S. *The Inhomogeneity of Plastic Deformation, American Society for Metals*; Metals Park: Materials Park, OH, USA, 1971; Chapter 2.
12. Smidt, F.A., Jr. *Dislocation Channeling in Irradiated Metals*; NRL Report 7078; Naval Research Laboratory: Washington, D.C., USA; 3; June; 1970.
13. Lu, B.T. Pitting and stress corrosion cracking behavior in welded austenitic stainless steel. *Electrochim. Acta* **2005**, *50*, 1391–1403. [CrossRef]
14. Nishimoto, K.; Ogawa, K. Corrosion properties in weldments of stainless steels (1). Metallurgical factors affecting corrosion properties. *Weld. Int.* **1999**, *13*, 845–854. [CrossRef]
15. Gooch, T.G. Corrosion behavior of welded stainless steel. *Weld. J. Incl. Weld. Res. Suppl.* **1996**, *75*, 135s–154s.
16. Brooks, J.A.; Thompson, A.W. Microstructural development and solidification cracking susceptibility of austenitic stainless steel welds. *Int. Mater. Rev.* **1991**, *36*, 16–44. [CrossRef]
17. Bilmes, P.; Gonzalez, A.; Llorente, C.; Solari, M. Effect of δ ferrite solidification morphology of austenitic stainless steel weld metal on properties of welded joints. *Weld. Int.* **1996**, *10*, 797–808. [CrossRef]
18. Allen, D.J. Solidification sequences in austenitic steel weld metal deposited on ferritic base material. *Met. Technol.* **1983**, *10*, 24–27. [CrossRef]

19. Pascual, M.; Salas, F.; Carcel, F.J.; Perales, M.; Sánchez, A. TIG AISI-316 welds using an inert gas welding chamber and different filler metals: Changes in mechanical properties and microstructure. *Rev. Met.* **2010**, *46*, 493–498. [CrossRef]
20. Carcel-Carrasco, J.; Pascual-Guillamon, M.; Perez-Puig, M. Microstructural characteristics and resistance to corrosion in welds of steel AISI 304 with inconel 625 exposed to ionizing radiation (radiation x). *DYNA Septiembre* **2014**, *89*, 542–551. [CrossRef]